

¹²³Sb-NQR study of unconventional superconductivity in the filled skutterudite heavy-fermion compound PrOs₄Sb₁₂ under high pressure up to 3.82 GPa

S. Kawasaki,^{1,*} K. Katayama,¹ H. Sugawara,² D. Kikuchi,³ H. Sato,³ and Guo-qing Zheng¹

¹Department of Physics, Okayama University, Okayama 700-8530, Japan

²Department of Mathematical and Natural Sciences, Faculty of Integrated Arts and Sciences, The University of Tokushima, Tokushima 770-8502, Japan

³Department of Physics, Graduate School of Science, Tokyo Metropolitan University, Hachioji, Tokyo 192-0397, Japan

(Received 4 June 2008; published 12 August 2008)

We report ¹²³Sb nuclear-quadrupole-resonance (NQR) measurements of the filled skutterudite heavy-fermion superconductor PrOs₄Sb₁₂ under high pressure. The temperature dependence of NQR frequency and the spin-lattice relaxation rate $1/T_1$ indicate that the crystal-electric-field splitting Δ_{CEF} between the ground-state Γ_1 singlet and the first-excited-state $\Gamma_4^{(2)}$ triplet decreases with increasing pressure. ac-susceptibility measurements indicate that the superconducting transition temperature (T_c) also decreases with increasing pressure. However, above $P \sim 2$ GPa, both Δ_{CEF} and T_c do not depend on external pressure up to $P = 3.82$ GPa. These pressure dependences of Δ_{CEF} and T_c suggest an intimate relationship between quadrupole excitations associated with the $\Gamma_4^{(2)}$ level and unconventional superconductivity in PrOs₄Sb₁₂. In the superconducting state, $1/T_1$ below $T_c = 1.55$ and 1.57 K at $P = 1.91$ and 2.63 GPa shows a power-law temperature variations and is proportional to T^5 at temperatures considerably below T_c . These data can be well fitted by the gap model $\Delta(\theta) = \Delta_0 \sin \theta$, with $\Delta_0 = 3.08k_B T_c$ and $3.04k_B T_c$ for $P = 1.91$ and 2.63 GPa, respectively. The results indicate that there exist point nodes in the gap function.

DOI: [10.1103/PhysRevB.78.064510](https://doi.org/10.1103/PhysRevB.78.064510)

PACS number(s): 74.62.Fj, 74.70.Tx, 76.60.Gv, 71.27.+a

I. INTRODUCTION

The filled skutterudite compound PrOs₄Sb₁₂ is the first praseodymium (Pr)-based heavy-fermion superconductor with superconducting transition temperature $T_c = 1.85$ K.^{1,2} The heavy-electron mass was found by the large electronic specific-heat coefficient $\gamma = 310\text{--}750$ mJ/(K² mol) (Refs. 1–3) and the de Haas–van Alphen effect measurement.⁴ It is confirmed that the crystal-electric-field (CEF) ground state for a Pr³⁺ ion is a Γ_1 singlet. Notably, the first-excited state of the $\Gamma_4^{(2)}$ triplet state is separated from ground state of Γ_1 singlet by a small gap of $\Delta_{\text{CEF}}/k_B \sim 10$ K.^{5–10} Because of this small Δ_{CEF} , the relation between the quadrupole fluctuations associated with the $\Gamma_4^{(2)}$ state^{6,11} and the occurrence of the unconventional superconductivity has been the focus of discussions.^{10,12,13}

The superconducting gap function is important for understanding the mechanism of unconventional superconductivity in PrOs₄Sb₁₂. First nuclear-quadrupole-resonance (NQR) measurement has revealed the uncommon nature of the superconductivity.¹⁴ The spin-lattice relaxation rate $1/T_1$ shows no coherence peak just below T_c ; nonetheless, it follows an exponential temperature dependence below T_c . Following this, a lot of experimental and theoretical works have been done to clarify the origin of uncommon superconductivity in PrOs₄Sb₁₂.^{15–34} However, the gap structure for superconductivity in PrOs₄Sb₁₂ has not yet been determined thus far.

Our previous NQR studies on the substitution system Pr(Os_{1-x}Ru_x)₄Sb₁₂ and PrOs₄Sb₁₂ at $P = 1.91$ GPa strongly suggested the existence of point nodes in the superconducting gap function, since Ru doping at the Os site in PrOs₄Sb₁₂ as a nonmagnetic impurity induces a residual density of states (DOS) in the superconducting gap³⁵ and $1/T_1$ below

$T_c(P)$ is proportional to T^5 considerably below T_c at $P = 1.91$ GPa, which is well fitted by the gap model $\Delta(\theta) = \Delta_0 \sin \theta$ with $\Delta_0 = 3.08k_B T_c$.³⁶ However, since the pressure dependence of $1/T_1$ below $T_c(P)$ is still not confirmed yet, further NQR studies under pressure have been deserved to determine the superconducting gap structure and to obtain further information on the relation between superconducting property and the quadrupole/magnetic fluctuations associated by the $\Gamma_4^{(2)}$ triplet state.

In this paper, we report on the extensive ¹²³Sb-NQR study of PrOs₄Sb₁₂ under high pressure up to $P = 3.82$ GPa and low temperatures. Applying pressure reduces T_c (Ref. 2) and may also change Δ_{CEF} (Ref. 37) and therefore can provide further information on the symmetry of the superconducting gap as well as on the mechanism of the superconductivity. We find that Δ_{CEF} and T_c decrease with increasing pressure but become almost constant above $P \sim 2$ GPa up to 3.82 GPa. These pressure dependences of Δ_{CEF} and T_c indicate an intimate relationship between quadrupole fluctuations and superconductivity. At $P = 1.91$ GPa and 2.63 GPa, $1/T_1$ decreases in proportion to T^5 at very low temperatures. This strongly evidences that there are point nodes in the superconducting gap function.

II. EXPERIMENTAL PROCEDURES

Single crystals of PrOs₄Sb₁₂ were grown by the Sb-flux method. For NQR measurements, the coarse powdered single crystals are used to allow the rf magnetic field to penetrate into the sample. The hydrostatic pressure was applied by utilizing NiCrAl/BeCu piston-cylinder-type cell for $P \leq 3$ GPa and indenter-type clamping cell³⁸ for $P \geq 3$ GPa, filled with Si oil and Daphne 7373 as a pressure-transmitting

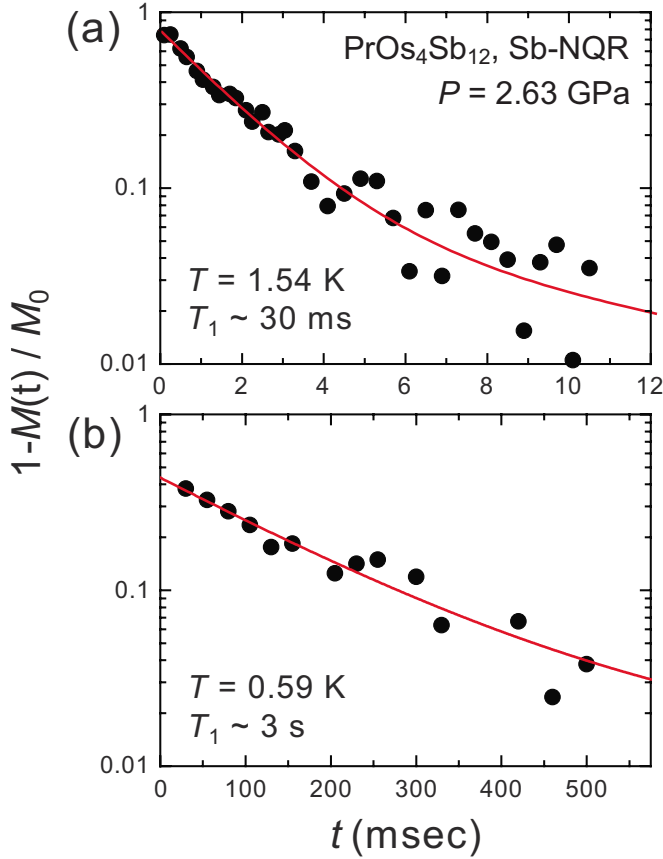


FIG. 1. (Color online) Recovery curves of the nuclear magnetization measured at $2\nu_Q$ transition of ^{123}Sb in $\text{PrOs}_4\text{Sb}_{12}$ at (a) $T = 1.54$ K [just below $T_c(P) = 1.57$ K] and (b) $T = 0.59$ K [considerably below $T_c(P)$] at $P = 2.63$ GPa. The solid curves are theoretical fitting curve (see text).

medium, respectively.^{39,40} The pressure at low temperatures was determined from the pressure dependence of the T_c values of Sn and/or Pb metals measured by a conventional four-terminal method. Temperature dependence of ac susceptibility is measured by a four-terminal method using NQR coil. Data below 1.4 K were collected using a $^3\text{He}/^4\text{He}$ dilution refrigerator at $P = 0$ and a ^3He refrigerator under $P = 1.91$ and 2.63 GPa, respectively.

The Sb nuclei have two isotopes of ^{121}Sb and ^{123}Sb with natural abundances of 57.3% and 42.7%, respectively. Since ^{121}Sb and ^{123}Sb have the nuclear spin $I = 5/2$ and $7/2$, respectively, five Sb-NQR transitions are observed.¹⁴ It has been confirmed that relaxation process at the Sb site is magnetic in origin.¹⁴ In the present experiment, all measurements were done at the $\pm 3/2 \leftrightarrow \pm 5/2$ transition (hereafter, $2\nu_Q$ transition for short) of the ^{123}Sb nucleus.

Figures 1(a) and 1(b) show a typical data set of ^{123}Sb -NQR recovery curves of $2\nu_Q$ transition to obtain relaxation time T_1 which are measured at $T = 1.54$ K just below $T_c(P) = 1.57$ K [Fig. 1(a)] and $T = 0.59$ K well below $T_c(P)$ [Fig. 1(b)] at $P = 2.63$ GPa, respectively. Since there is an asymmetry parameter η at the position of Sb nucleus, T_1 is determined by the theoretical curve of nuclear magnetization where the value of η is incorporated.⁴¹ As seen in Fig. 1(b), to avoid possible heating due to the rf pulses, we used small

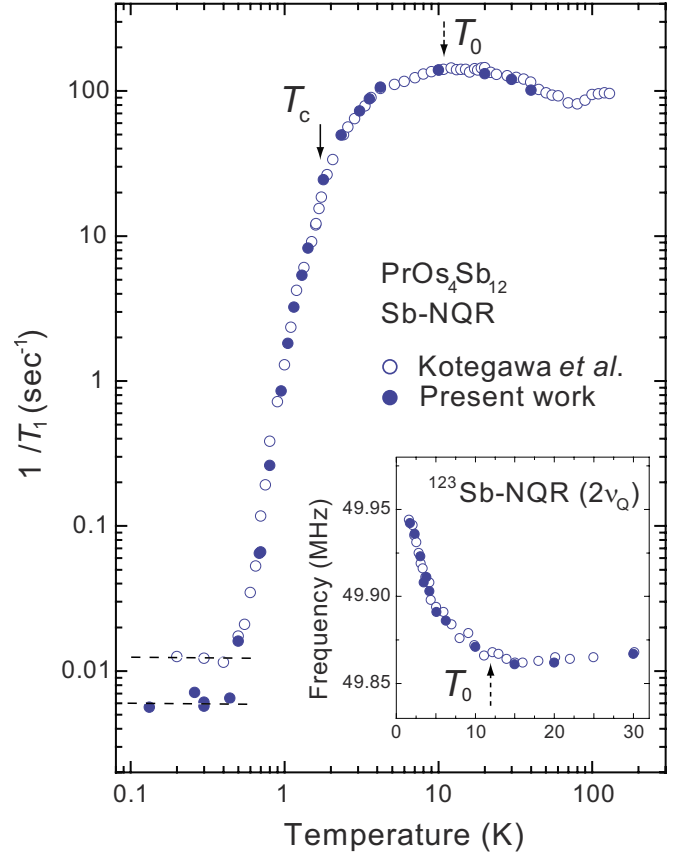


FIG. 2. (Color online) Temperature dependence of $1/T_1$ at $P = 0$ (solid circles) along with the data cited from literature (Ref. 14) (open circles). Dotted lines indicate a relation of $1/T_1 = \text{const}$. Solid and dotted arrows indicate T_c and T_0 , respectively. The inset shows temperature dependence of NQR frequency for $2\nu_Q$ transition at ambient pressure (solid circle) along with previous report (open circle) cited from literature (Ref. 14).

amplitude rf pulses in the T_1 measurements at very low temperatures. We confirmed the lack of a heating effect to T_1 process by ensuring that the spin-echo intensity is not affected by an rf pulse with a slightly off-resonance frequency, which was applied before the $\pi/2$ - π pulse sequence.

III. UNCOMMON SUPERCONDUCTIVITY IN $\text{PrOs}_4\text{Sb}_{12}$ AT AMBIENT PRESSURE

Figure 2 shows the temperature dependences of $1/T_1$ at ambient pressure (solid circles). The ambient-pressure data are in excellent agreement with those reported previously (open circles).¹⁴ At high temperatures, $100 \text{ K} > T > T_0 \sim 10$ K, $1/T_1$ increase slightly and become temperature independent with decreasing temperature. In this case, the relaxation rate is dominated by the Pr $4f^2$ -derived localized magnetic moments on the $\Gamma_4^{(2)}$ triplet state. With decreasing temperature below $T_0 \sim 10$ K, $1/T_1$ starts to decrease because a depopulation of $4f$ electron at $\Gamma_4^{(2)}$ triplet state occurs below $T \leq \Delta_{\text{CEF}}/k_B$. Such a phenomenon is also confirmed in temperature dependence of $2\nu_Q$ resonance frequency as will be discussed later. Remarkably, just below T_c , the Hebel-

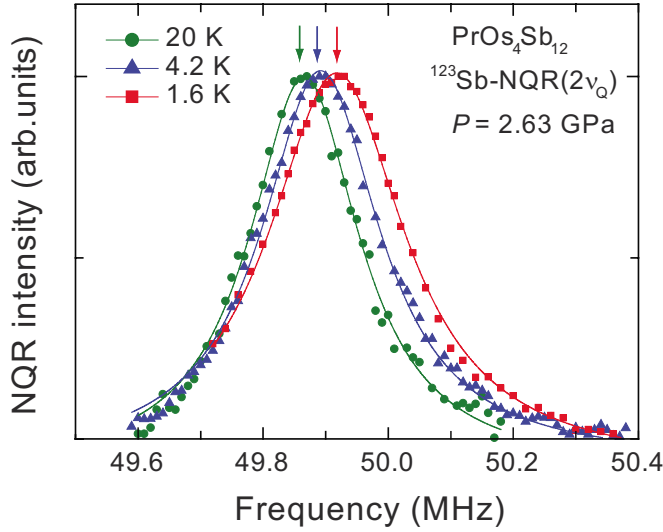


FIG. 3. (Color online) Temperature dependence of $2\nu_Q$ - ^{123}Sb -NQR spectra for $\text{PrOs}_4\text{Sb}_{12}$ at $P=2.63$ GPa. Solid curves are results of Lorentzian fittings. Solid arrows indicate peak positions.

Slichter (coherence) peak is absent, indicating a non- s -wave superconductivity. At further low temperatures $1/T_1$ decreases exponentially.¹⁴ Below $T=0.4$ K, $1/T_1$ become a constant, which is likely due to impurities. The present sample reproduces the previous results but shows smaller contribution of $1/T_1=\text{const}$ behavior at the lowest-temperature region than previous report,¹⁴ which suggests that now samples have better quality.²⁴ The most likely cause for such T -independent $1/T_1$ is the presence of a small amount of magnetic impurity, which is pressure independent.

The inset of Fig. 2 shows the temperature dependence of the $2\nu_Q$ transition at $P=0$. T_0 is the temperature at which the $2\nu_Q$ resonance frequency increases abruptly. Since the electrical field gradient (EFG) is predominantly determined by the on-site charge distribution, the NQR frequency is a powerful probe of the population of the ground/excited state. Indeed, in both $\text{PrOs}_4\text{Sb}_{12}$ (Ref. 14) and $\text{PrRu}_4\text{Sb}_{12}$,⁴² T_0 is in good agreement with Δ_{CEF}/k_B . More recently, it has been suggested that the temperature dependence of NQR frequency can be accounted for by the EFG associated with the hexadecapole moment of the $\Gamma_4^{(2)}$ state.⁴³ Therefore, it is concluded that the increase in the NQR frequency below T_0 is due to the depopulation of f electron in the $\Gamma_4^{(2)}$ state below this temperature. Here, we determined $T_0=12$ K at ambient pressure, below which $1/T_1$ and $d\nu_Q/dT$ starts to decrease.

IV. PRESSURE DEPENDENCE OF Δ_{CEF} IN $\text{PrOs}_4\text{Sb}_{12}$

As discussed in Sec. III, we can estimate a value of Δ_{CEF} from the temperature dependence of NQR frequency. Figure 3 shows typical data set of temperature dependence of ^{123}Sb -NQR spectra measured at $2\nu_Q$ transition at $P=2.63$ GPa. As seen in Fig. 3, at $P=2.63$ GPa, ^{123}Sb -NQR spectrum has a symmetrical shape and the center of spectrum clearly shifts to higher frequency due to the depopulation of f electron in the $\Gamma_4^{(2)}$ state below T_0 ($\propto \Delta_{\text{CEF}}/k_B$). Thus, we

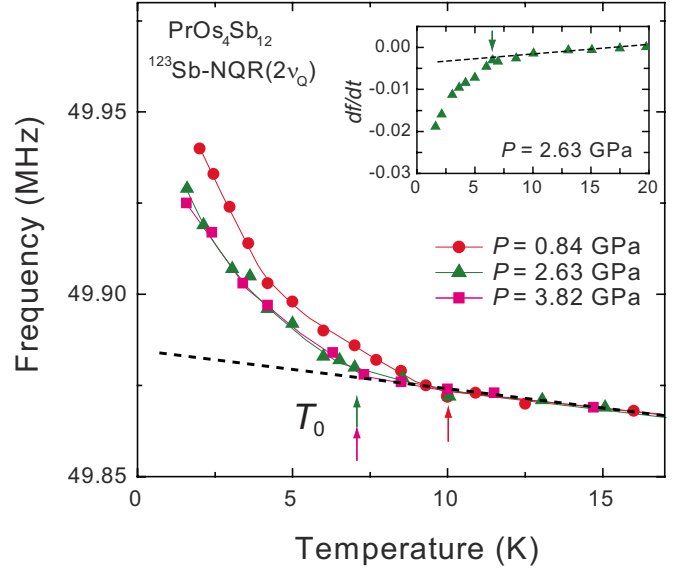


FIG. 4. (Color online) Temperature dependence of resonance frequency of $2\nu_Q$ transition at $P=0.84$ GPa (solid circles), 2.63 GPa (solid triangles), and 3.82 GPa (solid squares). The inset shows temperature dependence of df/dT at $P=2.63$ GPa. f denotes $2\nu_Q$ resonance frequency. Dotted lines are guides for the eyes. Solid arrows point to T_0 (see text).

can determine the peak position of NQR spectra precisely even under high pressure. Figure 4 summarizes the temperature dependence of $2\nu_Q$ resonance frequency under various pressures. The temperature dependence of $2\nu_Q$ resonance frequency shifts to lower temperature under pressure indicating the decrease in Δ_{CEF} with increasing pressure but it does not change between $P=2.63$ and 3.82 GPa. As seen in the inset of Fig. 4, we define T_0 at which df/dT starts to decrease steeply. Here, f denotes $2\nu_Q$ resonance frequency. We determined $T_0(P) \sim 10, 7, \text{ and } 7$ K at $P=0.84, 2.63, \text{ and } 3.82$ GPa, respectively. The pressure dependence of T_0 is summarized in Fig. 6(a). Notably, it is found that T_0 decreases with increasing pressure up to $P \sim 2$ GPa (Ref. 36) but becomes pressure independent above $P \sim 2$ GPa.

V. PRESSURE DEPENDENCE OF T_c IN $\text{PrOs}_4\text{Sb}_{12}$

Next, we turn to pressure dependence of T_c in $\text{PrOs}_4\text{Sb}_{12}$. Figure 5 shows temperature dependence of ac susceptibility at $P=0, 0.84, 1.91, \text{ and } 2.63$ GPa (main panel) measured using NQR coil in piston-cylinder-type pressure cell and $P=3.82$ GPa (inset) measured in indenter-type cell, respectively. As seen in the figure, the onset of superconducting diamagnetism is clearly observed at all pressures. From the onset of the superconducting diamagnetism, we determined $T_c(P)=1.87, 1.73, 1.55, 1.57, 1.57, \text{ and } 1.48$ K at $P=0, 0.84, 1.91, 2.34, 2.63, \text{ and } 3.82$ GPa, respectively. The pressure dependence of T_c is summarized in Fig. 6(b). T_c in $\text{PrOs}_4\text{Sb}_{12}$ decreases with increasing pressure.³⁶ However, it saturates above $P=2$ GPa. Notably, this pressure dependence of T_c is quite similar to the pressure dependence of T_0 [see Fig. 6(a)], which suggests an intimate relationship between Δ_{CEF} and

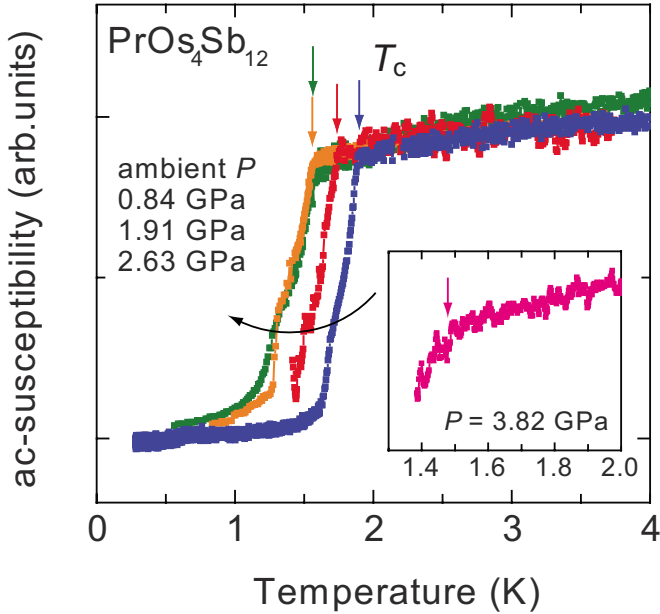


FIG. 5. (Color online) Temperature dependence of ac susceptibility at $P=0, 0.84, 1.91,$ and 2.63 GPa. The inset shows an onset of superconductivity at $P=3.82$ GPa. Arrows indicate $T_c(P)$.

the superconductivity in $\text{PrOs}_4\text{Sb}_{12}$. To clarify their relationship more quantitatively, further experimental studies under high pressure are highly deserved.

On the theoretical side, it has been proposed that the superconductivity is mediated by the excitons due to the $\Gamma_4^{(2)} - \Gamma_1$ quasiquartet.¹² In such case, $T_c(P)$ would increase due to the enhancement of such interaction when Δ_{CEF} is reduced. However, clearly, our results indicate T_c decreases with increasing pressure and do not lend a straightforward support to the theory. Notably, recent Eliashberg theory revealed the Δ_{CEF} dependence of T_c in $\text{La}_{1-x}\text{Pr}_x\text{Os}_4\text{Sb}_{12}$ system.³⁴ They indicate, in $\text{PrOs}_4\text{Sb}_{12}$, the reduction in Δ_{CEF} results a suppression of T_c due to the magnetic scattering. It is good agreement with present results. However, they also suggest that $\text{PrOs}_4\text{Sb}_{12}$ is s -wave singlet superconductor³⁴ and is not compatible with present results. Further theories are called for.

VI. EVOLUTION OF NORMAL STATE ELECTRIC PROPERTIES IN $\text{PrOs}_4\text{Sb}_{12}$ UNDER PRESSURE

Next, we discuss the pressure and temperature dependences of ^{123}Sb -NQR relaxation rate $1/T_1$, which gives information on the dynamical electric and on superconducting properties. Figure 7 shows the temperature dependence of $1/T_1T$ at $P=0, 1.91, 2.34,$ and 2.63 GPa. In Sec. IV, we concluded that Δ_{CEF} decreases with increasing pressure and it saturates above 2 GPa. Such a conclusion is also supported by the temperature dependence of $1/T_1T$ under pressure. The pressure effect appears below 4 K. At $P=0$, the reduction in $1/T_1T$ results in a peak structure in the plot of $1/T_1T$ versus T , which is due to the depopulation of the $\Gamma_4^{(2)}$ state below T_0 .¹⁴ At high pressures, $1/T_1T$ continues to increase and the decreases in $1/T_1T$ occur at lower temperature, indicating the

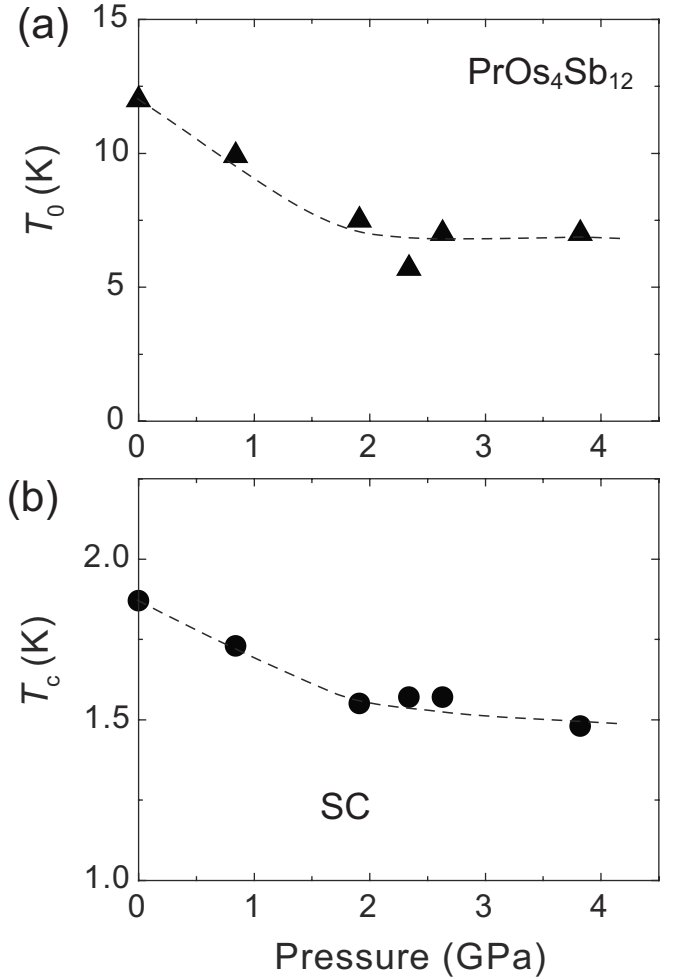


FIG. 6. Pressure-temperature phase diagrams for $\text{PrOs}_4\text{Sb}_{12}$ for T_0 [solid triangles in (a)] and T_c [solid circles in (b)] determined by present results. Dotted curves are guides for the eyes.

decrease in Δ_{CEF} . Since Δ_{CEF} decreases with increasing pressure, this may induce the increase in quadrupole fluctuations due to the f electron at the $\Gamma_4^{(2)}$ state. These results are consistent with the conclusion inferred from the magnetization measurement.³⁷ At $P=2.34$ and 2.63 GPa, $1/T_1T$ in the whole temperature regions has almost the same value. Thus, the peak position and T_c found in the temperature dependence of $1/T_1T$ are unchanged above $P \sim 2$ GPa, and these are consistent with the pressure dependence of T_0 and T_c determined by the temperature dependences of $2\nu_Q$ transition and ac susceptibility as discussed in Secs. I–V.

VII. SUPERCONDUCTING PROPERTIES UNDER PRESSURE

Next, we discuss the superconducting property in $\text{PrOs}_4\text{Sb}_{12}$ under pressure. Figure 8 shows the temperature dependence of $1/T_1$ at $P=0, 1.91,$ and 2.63 GPa. As discussed in Sec. III, the $1/T_1$ is T independent above T_0 , indicating that the relaxation in the high-temperature region is dominated by the $\text{Pr } 4f^2$ -derived localized magnetic moments.³⁶ With decreasing temperature below T_0 , $1/T_1$

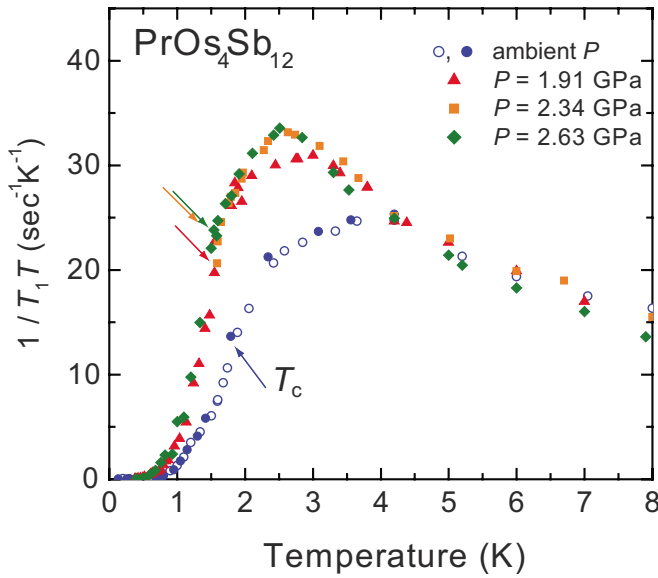


FIG. 7. (Color online) Temperature dependences of ¹²³Sb-NQR $1/T_1T$ for $\text{PrOs}_4\text{Sb}_{12}$ at $P=0$ (solid circles), $P=1.91$ GPa (solid triangles), $P=2.34$ GPa (solid squares), and $P=2.63$ GPa (solid diamonds) along with the data at ambient pressure cited from Ref. 14 (open circles). Solid arrows indicate $T_c(P)$.

starts to decrease. At $P=1.91$ and 2.63 GPa, the reduction in $1/T_1$ below T_0 to T_c becomes smaller compared to ambient-pressure data since the contribution of the excitation gap Δ_{CEF} in $1/T_1$ becomes smaller under pressure. Notably, just

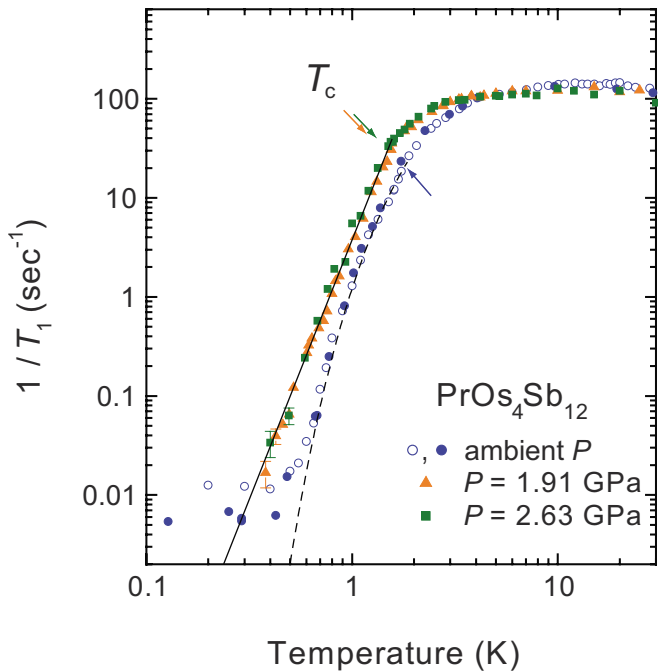


FIG. 8. (Color online) Temperature dependence of Sb-NQR $1/T_1$ at $P=0$ (solid circles), $P=1.91$ GPa (solid triangles), and $P=2.63$ GPa (solid squares) along with the data at ambient pressure cited from Ref. 14 (open circles). The straight line is a guide for the eyes. The dotted curve depicts the relation $1/T_1 \propto \exp(-\Delta_0/k_B T_c)$ with $\Delta_0/k_B T_c = 3.45$, proposed by Yogi *et al.* (Ref. 42). Arrows indicate T_c .

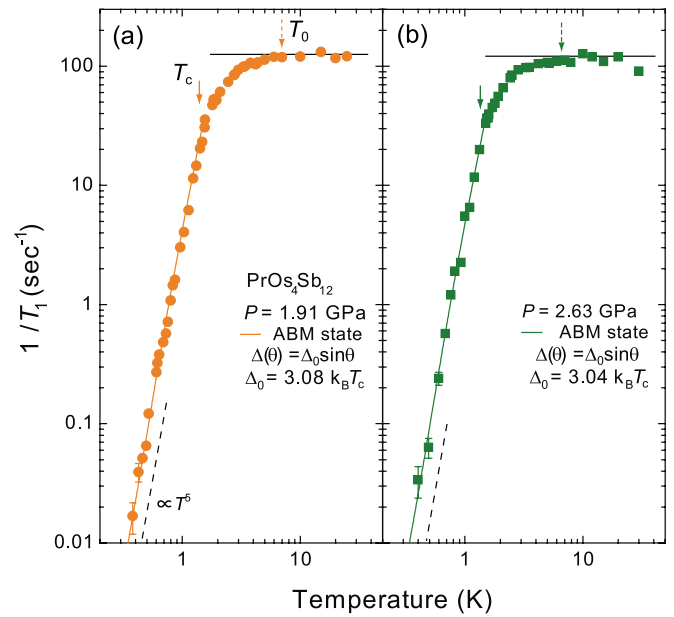


FIG. 9. (Color online) (a) Temperature dependence of $1/T_1$ at $P=1.91$ GPa [solid circles in (a)] and $P=2.63$ GPa [solid squares in (b)]. Solid and dotted arrows indicate T_c and T_0 , respectively. The solid curves are fit assuming the ABM state (see text). The solid and dotted lines indicate the relation of $1/T_1 \propto \text{constant}$ at high-temperature region and $1/T_1 \propto T^5$ well below T_c , respectively.

below $T_c(P)$, no coherence peak is observed at high pressures, even though T_c differs in each pressures. This indicates that the lack of coherence peak in $\text{PrOs}_4\text{Sb}_{12}$ is intrinsic property.

The temperature dependences of $1/T_1$ below $T_c(P)$ at high pressures are markedly different from that at ambient pressure. As seen in solid line in Fig. 8, $1/T_1$ at $P=1.91$ and 2.63 GPa decreases in a power law like temperature dependence below $T_c(P)$. However, at ambient pressure, $1/T_1$ decreases exponentially as indicated by dotted line in Fig. 8. What is the origin of these different temperature dependences of $1/T_1$ below T_c at ambient and under pressures? One possible scenario is provided below. At ambient pressure, the larger excitation gap Δ_{CEF} contributes to the reduction in $1/T_1$ below T_c , which make the temperature dependence of $1/T_1$ exponential like across T_c . Actually, at $P=1.91, 2.34,$ and 2.63 GPa, the anomaly at $T_c(P)$ in temperature dependence of $1/T_1$ becomes clearer compared to ambient-pressure data since the Δ_{CEF} decreases under pressure and its contribution to $1/T_1$ under pressure becomes smaller. So, we can determine $T_c(P)$ from the temperature dependence of $1/T_1$ as seen in Figs. 8 and 9. Such a scenario is also supported by our previous NQR studies in the substitution systems $\text{Pr}(\text{Os}_{1-x}\text{Ru}_x)_4\text{Sb}_{12}$.³⁵ It was confirmed that Δ_{CEF} becomes larger when Ru is substituted for Os site.^{22,35} As a result, in $\text{Pr}(\text{Os}_{1-x}\text{Ru}_x)_4\text{Sb}_{12}$, it becomes more difficult to determine T_c in the temperature dependence of $1/T_1$ compared to $\text{PrOs}_4\text{Sb}_{12}$ due to the increase in the contribution of excitation gap Δ_{CEF} in $1/T_1$ across T_c .³⁵ Thus, it is suggested that the excitation gap $\Delta_{\text{CEF}}/k_B \geq 10$ K may make temperature dependence of $1/T_1$ look unusual.

Notably, at $P=1.91$ and 2.63 GPa, $1/T_1$ become proportional to T^5 below $T \sim 0.6$ K. We find that a point-node

model, with a low-energy (E) superconducting DOS proportional to E^2 , can explain well these temperature dependences of $1/T_1$ below $T_c(P)$. As plotted in Figs. 9(a) and 9(b) by solid curves, we obtained excellent agreement with experimental results below $T_c(P)$. Here, we employed Anderson-Brinkmann-Morel (ABM) p -wave model^{44,45} to represent temperature dependence of $1/T_1$ below $T_c(P)$ as

$$\frac{T_1(T_c)}{T_1} = \frac{2}{k_B T} \int \left(\frac{N_S(E)}{N_0} \right)^2 f(E)[1-f(E)]dE,$$

where $N_S(E)/N_0 = E/\sqrt{E^2 - \Delta^2}$ with $\Delta(\theta) = \Delta_0 \sin \theta$. From fitting results, we obtained $\Delta_0/k_B T_c = 3.08$ and 3.04 for $P = 1.91$ and 2.63 GPa, respectively. Since the superconducting transition temperatures at $P = 1.91$ and 2.63 GPa are almost same, the values of $\Delta_0/k_B T_c$ are very close in both pressures. Recently, the $p+h$ model²⁷ proposed to explain the results of thermal conductivity would give a T^3 -like dependence since the DOS at low E is linear in E and is therefore not compatible with our results of $1/T_1 \propto T^5$.

VIII. CONCLUSION

In this paper, we have presented extensive ¹²³Sb-NQR studies on the normal and superconducting states in filled skutterudite heavy-fermion superconductor PrOs₄Sb₁₂ under high pressure up to 3.82 GPa. From the temperature dependences of ¹²³Sb-NQR frequency and the spin-lattice relaxation rate $1/T_1$ under pressure, it is indicated that the crystal-electric-field splitting Δ_{CEF} between the ground-state Γ_1 singlet and the first-excited-state $\Gamma_4^{(2)}$ triplet decreases with

increasing pressure. However, further application of pressure above $P = 3$ GPa reveals that Δ_{CEF} does not change in $2 \text{ GPa} < P < 4 \text{ GPa}$. Concomitantly, similar pressure dependence is confirmed in the superconducting transition temperature $T_c(P)$. Although the origin of these pressure dependences of Δ_{CEF} and T_c is still unknown, it suggests that superconductivity in PrOs₄Sb₁₂ is closely related to the $\Gamma_4^{(2)}$ state. In the superconducting state at $P = 1.91$ and 2.63 GPa, $1/T_1$ shows no coherence peak just below $T_c(P)$, shows power-law temperature variations, and is proportional to at temperatures considerably below $T_c(P)$. These data can be well represented by the gap model $\Delta(\theta) = \Delta_0 \sin \theta$ with $\Delta_0 = 3.08 k_B T_c$ and $3.04 k_B T_c$ for $P = 1.91$ and 2.63 GPa, respectively. This evidences that superconductivity in PrOs₄Sb₁₂ has point nodes in the gap function.

These results indicate that quadrupole/magnetic fluctuations induced by $\Gamma_4^{(2)}$ triplet state may play a vital role for the occurrence of unconventional superconductivity in PrOs₄Sb₁₂. We believe that present results shed further light on the mechanism of unconventional superconductivity in this compound and will stimulate further theoretical works.

ACKNOWLEDGMENTS

We thank M. Nishiyama for contribution in constructing low-temperature NMR probe and H. Kotegawa and T. C. Kobayashi for their experimental help in high-pressure measurements using indenter-type cell. This work was supported in part by grants for scientific research from MEXT and JSPS.

*kawasaki@science.okayama-u.ac.jp

¹E. D. Bauer, N. A. Frederick, P.-C. Ho, V. S. Zapf, and M. B. Maple, Phys. Rev. B **65**, 100506(R) (2002).

²M. B. Maple, P.-C. Ho, V. S. Zapf, N. A. Frederick, E. D. Bauer, W. M. Yuhasz, F. M. Woodward, and J. W. Lynn, J. Phys. Soc. Jpn. **71**, Suppl., 23 (2002).

³R. Vollmer, A. Faißt, C. Pfleiderer, H. v. Löhneysen, E. D. Bauer, P.-C. Ho, V. Zapf, and M. B. Maple, Phys. Rev. Lett. **90**, 057001 (2003).

⁴H. Sugawara, S. Osaki, S. R. Saha, Y. Aoki, H. Sato, Y. Inada, H. Shishido, R. Settai, Y. Ōnuki, H. Harima, and K. Oikawa, Phys. Rev. B **66**, 220504(R) (2002).

⁵Y. Aoki, T. Namiki, S. Ohsaki, S. R. Saha, H. Sugawara, and H. Sato, J. Phys. Soc. Jpn. **71**, 2098 (2002).

⁶K. Tenya, N. Oeschler, P. Gegenwart, F. Steglich, N. A. Frederick, E. D. Bauer, and M. B. Maple, Acta Phys. Pol. B **34**, 995 (2003).

⁷T. Tayama, T. Sakakibara, H. Sugawara, Y. Aoki, and H. Sato, J. Phys. Soc. Jpn. **72**, 1516 (2003).

⁸M. Kohgi, K. Iwasa, M. Nakajima, N. Metoki, S. Araki, N. Bernhoeft, J. M. Mignot, A. Gukasov, H. Sato, Y. Aoki, and H. Sugawara, J. Phys. Soc. Jpn. **72**, 1002 (2003).

⁹K. Kuwahara, K. Iwasa, M. Kohgi, K. Kaneko, S. Araki, N. Metoki, H. Sugawara, Y. Aoki, and H. Sato, J. Phys. Soc. Jpn.

73, 1438 (2004).

¹⁰E. A. Goremychkin, R. Osborn, E. D. Bauer, M. B. Maple, N. A. Frederick, W. M. Yuhasz, F. M. Woodward, and J. W. Lynn, Phys. Rev. Lett. **93**, 157003 (2004).

¹¹E. D. Bauer, P.-C. Ho, M. B. Maple, T. Schauerer, D. L. Cox, and F. B. Anders, Phys. Rev. B **73**, 094511 (2006).

¹²M. Matsumoto and M. Koga, J. Phys. Soc. Jpn. **74**, 1686 (2005).

¹³K. Kuwahara, K. Iwasa, M. Kohgi, K. Kaneko, N. Metoki, S. Raymond, M.-A. Méasson, J. Flouquet, H. Sugawara, Y. Aoki, and H. Sato, Phys. Rev. Lett. **95**, 107003 (2005).

¹⁴H. Kotegawa, M. Yogi, Y. Imamura, Y. Kawasaki, G.-q. Zheng, Y. Kitaoka, S. Ohsaki, H. Sugawara, Y. Aoki, and H. Sato, Phys. Rev. Lett. **90**, 027001 (2003).

¹⁵D. E. MacLaughlin, J. E. Sonier, R. H. Heffner, O. O. Bernal, B.-L. Young, M. S. Rose, G. D. Morris, E. D. Bauer, T. D. Do, and M. B. Maple, Phys. Rev. Lett. **89**, 157001 (2002).

¹⁶Y. Aoki, A. Tsuchiya, T. Kanayama, S. R. Saha, H. Sugawara, H. Sato, W. Higemoto, A. Koda, K. Ohishi, K. Nishiyama, and R. Kadono, Phys. Rev. Lett. **91**, 067003 (2003).

¹⁷K. Izawa, Y. Nakajima, J. Goryo, Y. Matsuda, S. Osaki, H. Sugawara, H. Sato, P. Thalmeier, and K. Maki, Phys. Rev. Lett. **90**, 117001 (2003).

¹⁸E. E. M. Chia, M. B. Salamon, H. Sugawara, and H. Sato, Phys. Rev. Lett. **91**, 247003 (2003).

- ¹⁹H. Suderow, S. Vieira, J. D. Strand, S. Bud'ko, and P. C. Canfield, *Phys. Rev. B* **69**, 060504(R) (2004).
- ²⁰T. Goto, Y. Nemoto, K. Sakai, T. Yamaguchi, M. Akatsu, T. Yanagisawa, H. Hazama, K. Onuki, H. Sugawara, and H. Sato, *Phys. Rev. B* **69**, 180511(R) (2004).
- ²¹M.-A. Measson, D. Braithwaite, J. Flouquet, G. Seyfarth, J. P. Brison, E. Lhotel, C. Paulsen, H. Sugawara, and H. Sato, *Phys. Rev. B* **70**, 064516 (2004).
- ²²N. A. Frederick, T. A. Sayles, and M. B. Maple, *Phys. Rev. B* **71**, 064508 (2005).
- ²³G. Seyfarth, J. P. Brison, M.-A. Méasson, J. Flouquet, K. Izawa, Y. Matsuda, H. Sugawara, and H. Sato, *Phys. Rev. Lett.* **95**, 107004 (2005).
- ²⁴M. Yogi, T. Nagai, Y. Imamura, H. Mukuda, Y. Kitaoka, D. Kikuchi, H. Sugawara, Y. Aoki, H. Sato, and H. Harima, *J. Phys. Soc. Jpn.* **75**, 124702 (2006).
- ²⁵W. Higemoto, S. R. Saha, A. Koda, K. Ohishi, R. Kadono, Y. Aoki, H. Sugawara, and H. Sato, *Phys. Rev. B* **75**, 020510(R) (2007).
- ²⁶K. Maki, H. Won, P. Thalmeier, Q. Yuan, K. Izawa, and Y. Matsuda, *Europhys. Lett.* **64**, 496 (2003).
- ²⁷K. Maki, S. Haas, D. Parker, H. Won, K. Izawa, and Y. Matsuda, *Europhys. Lett.* **68**, 720 (2004).
- ²⁸K. Miyake, H. Kohno, and H. Harima, *J. Phys.: Condens. Matter* **15**, L275 (2003).
- ²⁹J. Goryo, *Phys. Rev. B* **67**, 184511 (2003).
- ³⁰M. Ichioka, N. Nakai, and K. Machida, *J. Phys. Soc. Jpn.* **72**, 1322 (2003).
- ³¹M. Koga, M. Matsumoto, and H. Shiba, *J. Phys. Soc. Jpn.* **75**, 014709 (2006).
- ³²T. R. Abu Alrub and S. H. Curnoe, *Phys. Rev. B* **76**, 054514 (2007).
- ³³T. R. Abu Alrub and S. H. Curnoe, *Phys. Rev. B* **76**, 184511 (2007).
- ³⁴Jun Chang, Ilya Eremin, Peter Thalmeier, and Peter Fulde, *Phys. Rev. B* **76**, 220510(R) (2007).
- ³⁵M. Nishiyama, T. Kato, H. Sugawara, D. Kikuchi, H. Sato, H. Harima, and G.-q. Zheng, *J. Phys. Soc. Jpn.* **74**, 1938 (2005).
- ³⁶K. Katayama, S. Kawasaki, M. Nishiyama, H. Sugawara, D. Kikuchi, H. Sato, and G.-q. Zheng, *J. Phys. Soc. Jpn.* **76**, 023701 (2007).
- ³⁷T. Tayama, T. Sakakibara, H. Sugawara, and H. Sato, *J. Phys. Soc. Jpn.* **75**, 043707 (2006).
- ³⁸T. C. Kobayashi, H. Hidaka, H. Kotegawa, K. Fujiwara, and M. I. Erements, *Rev. Sci. Instrum.* **78**, 023909 (2007).
- ³⁹A. S. Kirichenko, A. V. Kornilov, and V. M. Pudalov, *Instrum. Exp. Tech.* **48**, 813 (2005).
- ⁴⁰K. Murata, H. Yoshino, H. O. Yadav, Y. Honda, and N. Shirakawa, *Rev. Sci. Instrum.* **68**, 2490 (1997).
- ⁴¹J. Chepin and J. H. Ross, Jr., *J. Phys.: Condens. Matter* **3**, 8103 (1991).
- ⁴²M. Yogi, H. Kotegawa, Y. Imamura, G.-q. Zheng, Y. Kitaoka, H. Sugawara, and H. Sato, *Phys. Rev. B* **67**, 180501(R) (2003).
- ⁴³H. Tou, M. Doi, M. Sera, M. Yogi, H. Sugawara, R. Shiina, and H. Sato, *J. Phys. Soc. Jpn.* **74**, 2695 (2005).
- ⁴⁴P. W. Anderson and P. Morel, *Phys. Rev.* **123**, 1911 (1961).
- ⁴⁵P. W. Anderson and W. F. Brinkman, *Phys. Rev. Lett.* **30**, 1108 (1973).